Applied Physics Express

The Japan Society of Applied Physics

LETTER

Schottky contacts on ultra-high-pressure-annealed GaN with high rectification ratio and near-unity ideality factor

Applied Physics Express 16, 031006 (2023) LETTER
https://doi.org/10.35848/1882-0786/acc443

Schottky contacts on ultra-high-pressure-annealed GaN with high rectification ratio and near-unity ideality factor

Shane R. Stein[1], Dolar Khachariya[2], Seiji Mita[2], M. Hayden Breckenridge[3], James Tweedie[2], Pramod Reddy[2], Kacper Sierakowski[4], Grzegorz Kamler[4], Michał Boćkowski[4], Erhard Kohn[3], Zlatko Sitar[2,3], Ramón Collazo[3], and Spyridon Pavlidis[1*]

[1]Department of Electrical and Computer Engineering, North Carolina State University, Raleigh, NC 27695-7911, United States of America
[2]Adroit Materials, Inc., 2054 Kildaire Farm Road., Cary NC 27518, United States of America
[3]Department of Materials Science and Engineering, North Carolina State University, Raleigh, NC 27695-7919, United States of America
[4]Institute of High-Pressure Physics, Polish Academy of Sciences, Sokołowska 29/37, 01-142 Warsaw, Poland

*E-mail: spavlidis@ncsu.edu

Received February 19, 2023; revised March 8, 2023; accepted March 13, 2023; published online March 23, 2023

We investigate the electrical characteristics of Ni Schottky contacts on n-type GaN films that have undergone ultra-high-pressure annealing (UHPA), a key processing step for activating implanted Mg. Contacts deposited on these films exhibit low rectification and high leakage current compared to contacts on as-grown films. By employing an optimized surface treatment to restore the GaN surface following UHPA, we obtain Schottky contacts with a high rectification ratio of ~10^9, a near-unity ideality factor of 1.03, and a barrier height of ~0.9 eV. These characteristics enable the development of GaN junction barrier Schottky diodes employing Mg implantation and UHPA.

GaN is an exciting candidate for next-generation power semiconductor devices due to its wide bandgap and high critical electric field.[1,2] Power diodes and transistors have been reported with high breakdown voltage and low specific on-resistance (R_{ON}) nearing the theoretical material limits.[3–6] Moreover, with increasing substrate diameter and quality, vertical GaN power devices are becoming increasingly commercially viable.[7]

Prospective GaN power devices include the metal–oxide–semiconductor field-effect transistor,[5] junction field-effect transistor,[2,6] and junction barrier Schottky (JBS) diode.[8–10] These devices, as well as edge terminations such as junction termination extension or floating guarding rings necessary for high blocking voltage, require selective area doping. Ion implantation is an established method for selective area doping in other semiconductors, but its translation to GaN technology is challenging since GaN is prone to surface decomposition when annealed at the high temperatures necessary for dopant activation and damage recovery after implantation.[11] Ultra-high-pressure annealing (UHPA) is a recent post-implantation annealing technique that is able to prevent decomposition even without the need for a cap layer by applying an ultra-high N_2 overpressure in the range of 0.3–1 GPa to stabilize the GaN surface. Moreover, UHPA has demonstrated implanted Mg activation efficiencies near or equal to 100%,[12–15] substantially exceeding those of other techniques.[9,16–19] For JBS diodes, high-quality Schottky contacts must also be made to the n-type regions adjacent to the implanted p-GaN, and it is well-known that the electrical behavior of Schottky contacts is strongly dependent on the properties of the semiconductor surface, which can be sensitive to processing steps.[20,21] Therefore, to fabricate GaN JBS diodes with competitive performance via ion implantation and UHPA, it is critical to understand the electrical behavior of Schottky contacts formed on the annealed GaN surfaces and to be able to obtain ideal Schottky characteristics, particularly after annealing at 1300 °C, which is necessary for effective Mg activation.[12–15]

In this work, we investigate the electrical characteristics of Ni Schottky contacts on UHP annealed n-type GaN films via current–voltage (I–V) and capacitance–voltage (C–V) measurements. Hall effect and X-ray photoelectron spectroscopy (XPS) data are also analyzed to examine possible bulk- or surface-based factors that influence contact behavior. We then demonstrate Schottky contacts with high rectification ratio, near-unity ideality factor, and high homogeneity by using a surface treatment to recover the surface after UHPA prior to contact deposition, paving the way for high-performance ion-implanted vertical GaN JBS diodes, as we have recently reported elsewhere,[8] as well as other devices in the future which require selective area doping.[2]

1 μm thick n^--GaN epitaxial films were grown on ammonothermal n^+-GaN substrates using a vertical, cold-wall, radio frequency-heated, low-pressure metalorganic chemical vapor deposition (MOCVD) reactor.[22] Wafers were cleaved into 1 × 1 cm^2 pieces for different experimental splits. UHPA was performed at temperatures of 1100 °C–1300 °C for 20 min with 400 MPa or 1 GPa of N_2 overpressure.[12,15] After UHPA, some samples underwent a specially developed proprietary surface treatment to reconstruct the surface. UHP annealed samples with and without surface treatment, as well as reference samples without UHPA, were then cleaned in 10% buffered HF and 70 °C 1:1 $HCl:H_2O$. 70/70 nm thick Ni/Au Schottky contacts were deposited on the samples via e-beam evaporation for the anodes. Large-area Ti/Al/Ni/Au Ohmic contacts were deposited on the backside of the n^+-GaN substrate for the cathodes. Additional Schottky diodes were also fabricated on a 1.2 μm thick n^--GaN film grown on a sapphire substrate and diced into pieces for each experimental split. The fabrication procedure was the same for these samples as described above except that Ohmic contacts for the cathodes were formed on the top face of the samples due to the insulating substrate. These samples were also used for the XPS and Hall effect measurements.

Diode I–V and C–V measurements were conducted on-wafer using a probe station and Keithley 4200 semiconductor parameter analyzer. The C–V measurements used an ac voltage of 20 mV and a frequency of 1 MHz. Details of the XPS measurement procedure are described in previous

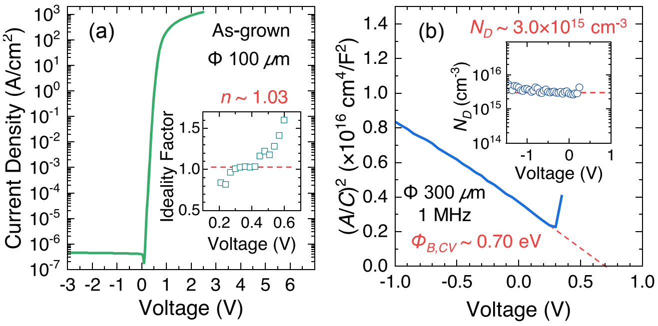

Fig. 1. (Color online) (a) *I–V* characteristics and extracted ideality factor of the Schottky contact on the as-grown GaN-on-GaN film without UHPA. (b) *C–V* characteristics and extracted net donor concentration and Schottky barrier height of a large-area contact on the same sample.

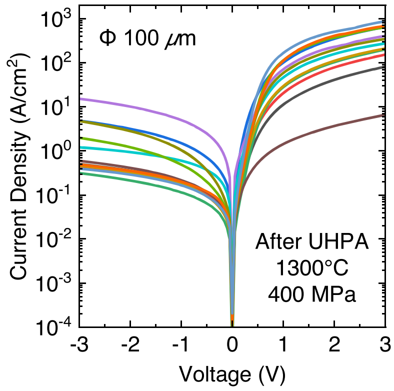

Fig. 2. (Color online) *I–V* characteristics of Schottky contacts on the UHP annealed GaN-on-GaN film.

works.[20,21] Hall effect measurements were performed on the GaN-on-sapphire samples with Ohmic contacts at the corners of the square samples in a van der Pauw geometry using an Ecopia DC Hall measurement system.

Figure 1(a) shows the measured *I–V* characteristics of a reference as-grown Schottky diode on GaN substrate with 100 μm circular contact diameter that is representative of all diodes on the sample. The diode exhibits a rectification ratio greater than 10^9 at ±2.5 V. The linearly extrapolated turn-on voltage (V_{ON}) from the *I–V* data is 0.71 V. An ideality factor (n) of 1.03 is measured, indicating that the Schottky characteristics are dominated by thermionic emission without significant influence of an interlayer dielectric, surface impurities, or other leakage paths. A plot of $1/C^2$–V for a 300 μm diameter diode at 1 MHz is shown in Fig. 1(b). A Schottky barrier height ($\Phi_{B,CV}$) of ∼0.70 eV is found by linearly extrapolating the $1/C^2$–V curve to zero. This barrier height is in agreement with other reports of near-ideal Ni Schottky contacts on n-type GaN[21] and consistent with the measured Fermi level pinning at GaN surfaces via XPS.[23] A net donor concentration (N_D) of $\sim 3.0 \times 10^{15}$ cm^{-3} in the epitaxial film is measured from the slope of the curve, which agrees with the expected net doping concentration from MOCVD. These data confirm the high quality of our reference Schottky contacts on as-grown GaN films.

Figure 2 shows the measured *I–V* characteristics of several 100 μm diameter Ni/Au Schottky contacts on the GaN-on-GaN film that was UHP annealed at 1300 °C and 400 MPa prior to contact deposition. The contacts exhibit high reverse and subthreshold leakage current, indicating the presence of alternative leakage paths. Large variation of forward and reverse diode current is measured across the wafer as well. The highest measured rectification ratio is $\sim 2 \times 10^3$ at ±3 V. The high leakage current rendered *C–V* measurements unreliable for extracting Φ_B and N_D, but the linearly extrapolated V_{ON} from the *I–V* curves is ∼0.5 V, lower than that of the as-grown reference diodes. The lowest measured n is ∼3.1, also due to the high subthreshold leakage.

In JBS diodes, the shielding of the n-type Schottky contact by the surrounding p-type grid reduces the electric field at the metal–semiconductor interface (E_m), lowering the Schottky leakage current resulting from barrier lowering and tunneling.[24] Yet the Schottky contact must still support the reduced E_m and the leakage current for this E_m must be low enough for use in power applications. E_m for the Schottky contacts without shielding is given by

$$E_m = \sqrt{\frac{2qN_D}{\varepsilon_s}(V_B - V_A)}, \quad (1)$$

where V_A is the applied voltage, V_B is the Schottky contact potential, ε_s is the permittivity of GaN, and q is electronic charge. According to this equation, assuming $V_B = 0.5$ V, $N_D = 3.0 \times 10^{15}$ cm^{-3}, and $\varepsilon_s = 9.5\varepsilon_0$, the E_m at $V_A = -1$ V is ∼0.04 MV cm^{-1}. The high measured reverse leakage current of ∼0.1 A cm^{-2} or higher at such low E_m is prohibitive for high-voltage JBS blocking capability and therefore requires substantial reduction.

To study possible sources for this contact degradation, XPS and Hall effect measurements were conducted on UHP annealed GaN films. As shown in Fig. 3, XPS on the GaN-on-sapphire sample UHP annealed at 1300 °C and 400 MPa gives a Ga:N molar ratio of 1.57 at the surface, which is slightly higher than our typical as-grown GaN surfaces (∼1.3),[20,23] but not altogether out of range for GaN films.[25] The O molar fraction at the surface is ∼8%, which is typical and corresponds to 0.5–1 monolayer of native oxide.[23] Table I shows the sheet carrier concentration (n_{sh}) measured via Hall effect for the as-grown and UHP annealed GaN-on-sapphire films for different UHPA temperatures and pressures. Note that the samples under study were cleaved from the same epitaxial wafer. The measured n_{sh} shows no increasing trend with annealing temperature or pressure, making it unlikely that donor impurity (e.g. O) diffusion into the films from the ambient (UHPA) environment is raising the donor concentration near the surface, making it a bulk effect. For this to happen, the donor concentration near the surface would need to be $\gg 1 \times 10^{18}$ cm^{-2}, while being confined to a thickness $<$ 10 nm for the sheet concentration to remain below the sample-to-sample variation of $\sim 1 \times 10^{12}$ cm^{-2} and therefore be undetectable by the Hall effect measurements. The slightly high Ga:N ratio instead suggests the possible presence of N vacancies at the surface, which could serve as donors and effectively comprise a thin n^+ region at the surface. Another possibility is the formation of a particular native oxide reconstruction during UHPA that pins the Fermi level to the conduction band,[26] lowering the Schottky barrier to virtually zero across the entire contact or patches of the contact region, enhancing leakage current.

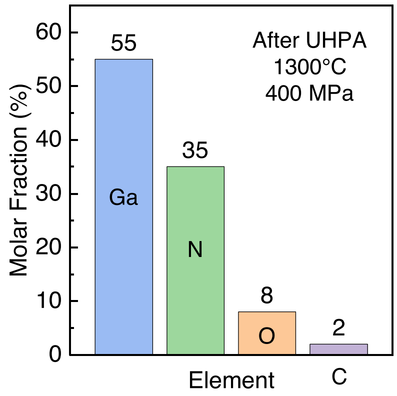

Fig. 3. (Color online) Molar fraction (%) of Ga, N, O, and C on surface of the UHP annealed GaN-on-sapphire film measured via XPS.

Table I. Sheet carrier concentration (n_{sh}) of the GaN-on-sapphire films under different UHPA conditions measured via Hall effect.

Annealing condition	n_{sh} (cm^{-2})
As-grown	5.7×10^{12}
1100 °C, 400 MPa	7.6×10^{12}
1200 °C, 400 MPa	4.5×10^{12}
1300 °C, 400 MPa	4.1×10^{12}
1300 °C, 1 GPa	3.8×10^{12}

These hypotheses imply that bulk degradation is not introduced by UHPA, and surface-based factors determine the contact behavior.

To counteract these effects, we employed a specially developed proprietary surface treatment in between the UHPA and metal deposition steps. As shown in Fig. 4(a), this results in a leakage current reduction of over 10^5 compared to the Schottky contacts on annealed films without the surface treatment, resulting in a similar leakage level as the contacts on as-grown films. This behavior is necessary to enable high-voltage blocking capability, for example in JBS diodes. The *I–V* characteristics exhibit a rectification ratio of $\sim 10^9$ at ±2.5 V and an n of 1.03, in excellent agreement with that measured on the as-grown reference diodes from the same wafer. Measuring several diodes showed that the *I–V* characteristics, including the rectification ratio and near-unity n, were repeatable, and those shown in Fig. 4(a) are representative of the sample. The *C–V* characteristics, shown in Fig. 4(b), give a net N_D of $\sim 3.3 \times 10^{15}\ cm^{-3}$, which is also in agreement with the as-grown diodes. The linearly-extrapolated V_{ON} from the *I–V* data is 0.85 V. *C–V* and variable-temperature *I–V* measurements[20] (Fig. 4(c)) give a Schottky barrier height of $\Phi_{B,CV} \sim 0.95$ eV and $\Phi_{B,IV} \sim 0.90$ eV, respectively. The small difference between $\Phi_{B,CV}$ and $\Phi_{B,IV}$ and the linear relationship between $\ln(I_0/AT^2)$ and T^{-1} in the Richardson plot indicate a highly homogenous Schottky barrier.[27,28] The barrier is ~0.2 eV higher than those obtained on the as-grown diodes. The presence of a thick oxide interlayer causing the increased barrier height compared to the as-grown diodes is precluded by the low ideality factor. Instead, it is more likely that the surface treatment after UHPA modifies or lowers the concentration of surface states so that the charge neutrality level is lowered compared to the as-grown surface, increasing Φ_B.[23] The demonstration of highly ideal Schottky contacts on UHP annealed n-GaN is a critical milestone achievement for the development of GaN devices requiring selective area doping,[2] and is a key enabling factor in our recent demonstration of record-performance vertical GaN JBS diodes fabricated via ion implantation and UHPA.[8]

In conclusion, Ni contacts deposited on n-type GaN following UHPA suffer from degraded Schottky characteristics, exhibiting high leakage current greater than 0.1 A cm^{-2}, which is prohibitive to the fabrication of JBS diodes capable of high blocking voltage. Hall effect measurements show no significant change in bulk doping concentration of the annealed films. XPS shows a slightly N-deficient surface, but the elemental molar fractions at the surface are otherwise in line with typical as-grown films. The source of leakage for the Schottky contacts thus appears confined to the surface due either to N vacancies or a native oxide reconstruction pinning the Fermi level to the conduction band. This was confirmed by the recovery of the surface after UHPA using a specially developed surface treatment. Ni contacts on the restored surface show highly homogeneous Schottky characteristics with a rectification ratio of $\sim 10^9$, an ideality factor of ~1.03, and a barrier height of ~0.9 eV, enabling the

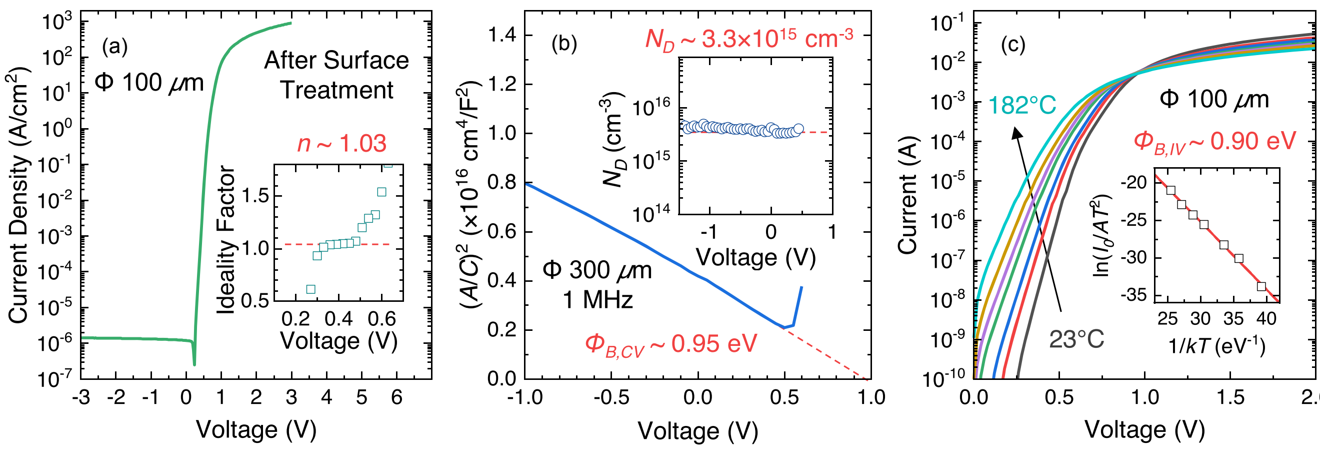

Fig. 4. (Color online) (a) *I–V* characteristics and extracted ideality factor of the Schottky contact deposited on the GaN-on-GaN film following UHPA and surface treatment. (b) *C–V* characteristics and extracted net donor concentration and Schottky barrier height of a large-area contact on the same sample. (c) *I–V* characteristics of the Schottky contact for temperatures ranging from 23 °C to 182 °C and extracted Richardson plot giving the Schottky barrier height.

fabrication of high-performance ion-implanted vertical GaN JBS diodes.

Acknowledgments The authors gratefully acknowledge funding in part from NSF (ECCS-1916800, ECCS-1508854, ECCS-1610992, DMR-1508191, ECCS-1653383), DOE (DE-AR0000873, DE-AR000149), ONRG NICOP (N62909–17–1-2004), NCBR (TECHMATSTRATEG-III/0003/2019-00), and NCSU faculty start-up fund. This work was performed in part at the NCSU Nanofabrication Facility (NNF) and Analytical Instrumentation Facility (AIF), which are supported by the State of North Carolina and the National Science Foundation (Award No. ECCS-1542015). The NNF and AIF are members of the North Carolina Research Triangle Nanotechnology Network (RTNN), a site in the National Nanotechnology Coordinated Infrastructure (NNCI).

ORCID iDs Dolar Khachariya https://orcid.org/0000-0002-8780-4583 Spyridon Pavlidis https://orcid.org/0000-0002-1690-2581

1) J. A. Cooper and D. T. Morisette, IEEE Electron Device Lett. **41**, 892 (2020).
2) S. R. Stein, D. Khachariya, and S. Pavlidis, Semicond. Sci. Technol. **37**, 125011 (2022).
3) L. Yates et al., IEEE Trans. Electron Devices **69**, 1931 (2022).
4) Y. Saitoh, K. Sumiyoshi, M. Okada, T. Horii, T. Miyazaki, H. Shiomi, M. Ueno, K. Katayama, M. Kiyama, and T. Nakamura, Appl. Phys. Express **3**, 081001 (2010).
5) T. Oka, I. Tsutomu, U. Yukihisa, and N. Junya, Appl. Phys. Express **8**, 054101 (2015).
6) J. Liu, M. Xiao, Y. Zhang, S. Pidaparthi, H. Cui, A. Edwards, L. Baubutr, W. Meier, C. Coles, and C. Drowley, 2020 IEEE Int. Electron Devices Meeting, 2020, 23.2.1.
7) R. Kucharski, T. Sochacki, B. Lucznik, and M. Bockowski, J. Appl. Phys. **128**, 050902 (2020).
8) D. Khachariya et al., Appl. Phys. Express **15**, 101004 (2022).
9) Y. H. Zhang et al., IEEE Electron Device Lett. **38**, 1097 (2017).
10) M. Matys, K. Kitagawa, T. Narita, T. Uesugi, J. Suda, and T. Kachi, Appl. Phys. Lett. **121**, 203507 (2022).
11) H. W. Choi, M. A. Rana, S. J. Chua, T. Osipowicz, and J. S. Pan, Semicond. Sci. Technol. **17**, 1223 (2002).
12) M. H. Breckenridge et al., Appl. Phys. Lett. **118**, 022101 (2021).
13) H. Sakurai et al., Appl. Phys. Lett. **115**, 142104 (2019).
14) K. Hirukawa, K. Sumida, H. Sakurai, H. Fujikura, M. Horita, Y. Otoki, K. Sierakowski, M. Bockowski, T. Kachi, and J. Suda, Appl. Phys. Express **14**, 056501 (2021).
15) K. Sumida, K. Hirukawa, H. Sakurai, K. Sierakowski, M. Horita, M. Bockowski, T. Kachi, and J. Suda, Appl. Phys. Express **14**, 121004 (2021).
16) T. Anderson, B. Feigelson, F. Kub, M. Tadjer, K. Hobart, M. Mastro, J. Hite, and C. Eddy Jr, Electron. Lett. **50**, 197 (2014).
17) V. Meyers et al., J. Appl. Phys. **128**, 085701 (2020).
18) S. R. Aid, T. Uneme, N. Wakabayashi, K. Yamazaki, A. Uedono, and S. Matsumoto, Phys. Status Solidi a **214**, 1700225 (2017).
19) T. Niwa, T. Fujii, and T. Oka, Appl. Phys. Express **10**, 091002 (2017).
20) D. Khachariya, D. Szymanski, R. Sengupta, P. Reddy, E. Kohn, Z. Sitar, R. Collazo, and S. Pavlidis, J. Appl. Phys. **128**, 064501 (2020).
21) P. Reddy, B. Sarkar, F. Kaess, M. Gerhold, E. Kohn, R. Collazo, and Z. Sitar, Appl. Phys. Lett. **110**, 011603 (2017).
22) S. Rathkanthiwar, P. Bagheri, D. Khachariya, S. Mita, S. Pavlidis, P. Reddy, R. Kirste, J. Tweedie, Z. Sitar, and R. Collazo, Appl. Phys. Express **15**, 051003 (2022).
23) P. Reddy, I. Bryan, Z. Bryan, W. Guo, L. Hussey, R. Collazo, and Z. Sitar, J. Appl. Phys. **116**, 123701 (2014).
24) B. J. Baliga, *Gallium Nitride and Silicon Carbide Power Devices* (World Scientific Publishing Company, Hackensack, NJ, 2016), Chap. 6.
25) H. S. Craft, A. L. Rice, R. Collazo, Z. Sitar, and J.-P. Maria, Appl. Phys. Lett. **98**, 082110 (2011).
26) K. J. Mirrielees, J. H. Dycus, J. N. Baker, P. Reddy, R. Collazo, Z. Sitar, J. M. LeBeau, and D. L. Irving, J. Appl. Phys. **129**, 195304 (2021).
27) J. H. Werner and H. H. Güttler, J. Appl. Phys. **69**, 1522 (1991).
28) R. T. Tung, Appl. Phys. Lett. **58**, 2821 (1991).